Calculated Infrared Absorption and Vibrational Circular Dichroism Intensities of Oxirane and Its Deuterated Analogues

R. Dutler and A. Rauk*

Contribution from the Department of Chemistry, The University of Calgary, Calgary, Alberta, Canada T2N 1N4. *Received January 27, 1989*

Abstract: An ab initio implementation of the vibronic coupling theory of Nafie and Freedman is described and applied to the computation of vibrational circular dichroism (VCD) intensities of (*S*)-2-deuteriooxirane, (*S*,*S*)-2,3-dideuteriooxirane, and (*S*)-2,2,3-trideuteriooxirane. The theory is found to reproduce the published spectral features of (*S*,*S*)-2,3-dideuteriooxirane very well if the basis set incorporates derivatives of the normal set of basis functions. A suitable basis set, based on the standard 6-31g set and designated 6-31$\tilde{g}$(-2$\tilde{s}$,2$\tilde{p}$,2$\tilde{p}_H$), is proposed. The 6-31$\tilde{g}$(-2$\tilde{s}$,2$\tilde{p}$,2$\tilde{p}_H$) basis set is found to yield a geometry for oxirane that is closer to the microwave structure than obtained by optimization with the comparably sized 6-31G** set. Uniform scaling or limited nonuniform scaling of the 6-31$\tilde{g}$(-2$\tilde{s}$,2$\tilde{p}$,2$\tilde{p}_H$) force constants permit excellent agreement (<1% error) with observed vibrational frequencies of oxirane and tetradeuteriooxirane. Quite satisfactory agreement with the measured IR intensities for these two compounds is also obtained. Scaling of the force constants in a nonuniform manner has a slightly adverse effect on calculated IR intensities, suggesting that the ab initio normal modes may be preferable. The APT theory of VCD intensities introduced by Nafie and Freedman has been tested against the vibronic coupling theory. Ab initio atomic polar tensors that accurately reproduce the IR spectrum of oxirane and the d_4 species were employed. The APT theory was found to have little predictive capability except possibly in the C-D and C-H stretching region of the spectrum. The full IR spectra of all of the deuterated isotopomers of oxirane and the VCD spectra of all of the chiral species are predicted.

Vibrational circular dichroism spectroscopy, in connection with the commonly used infrared absorption technique, is becoming established as an important method for the understanding of the interaction of infrared radiation with chiral molecules and for obtaining a wealth of structural information of such species. It is thus no surprise that over the years numerous accounts on experimental as well as theoretical infrared absorption and vibrational circular dichroism studies of a multitude of molecules have appeared in the chemical literature. Owing to their molecular size and the relative simplicity of the spectra, three- and four-membered ring systems have been the subject of many previous investigations from both experimental and theoretical perspectives in the infrared region of the light spectrum.[1-11] Of these, the chiral *trans*-2,3-dideuteriooxirane molecule is among the smallest species for which vibrational circular dichroism and concomitant infrared absorption has been measured, albeit data reported to date are restricted to the C-H and C-D stretching region of the molecule.[8-10] There have been numerous studies of the vibrational spectra of oxirane, the most recent of which are those by Cant and Armstead,[12] Bertie and Jacobs,[13] and Nakanaga.[14] Ab initio calculations on oxirane and/or oxirane-d_4 have been carried out by Komornicki et al.,[15] Hess et al.,[16] Lowe et al.,[17] and Simandiras et al.[18] The manageable size of the (deuterated) oxirane molecules allows a direct comparison between experiment and the most sophisticated ab initio infrared absorption and vibrational circular dichroism intensity calculation of some isotopomers of the parent oxirane molecule as reported in this article.

The theoretical treatment of both the infrared absorption and vibrational circular dichroism processes have been well documented in the literature by using a diversity of approaches.[11,19-31] Within the confinement of the Beer-Lambert law, the decadic molar extinction coefficient ϵ and the differential decadic molar extinction $\Delta\epsilon$ are directly related to the absorption and circular dichroism of an isotropic material, respectively. The corresponding integrated

(1) Plavarapu, P. L.; Michalska, D. F. *J. Am. Chem. Soc.* **1983**, *105*, 6190-6191.
(2) Polavarapu, P. L.; Michalska, D. F. *Mol. Phys.* **1984**, *52*, 1225-1235.
(3) Palavarapu, P. L.; Hess, Jr., B. A.; Schaad, L. J. *J. Chem. Phys.* **1985**, *82*, 1705-1710.
(4) (a) Annamalai, A.; Keiderling, T. A.; Chickos, J. S. *J. Am. Chem. Soc.* **1984**, *106*, 6254-6262. (b) Annamalai, A.; Keiderling, T. A.; Chickos, J. S. *J. Am. Chem. Soc.* **1985**, *107*, 2285-2291.
(5) Shaw, R. A. Ab Initio Force Fields, Vibrational Circular Dichroism and Model Calculations for two Methyl Substituted Oxetans. Ph.D. Thesis, University of Calgary, 1986.
(6) (a) Lowe, M. A.; Stephens, P. J.; Segal, G. A. *Chem. Phys. Lett.* **1986**, *123*, 108-116. (b) Lowe, M. A.; Segal, G. A.; Stephens, P. J. *J. Am. Chem. Soc.* **1986**, *108*, 248-256.
(7) Polavarapu, P. L.; Hess, Jr., B. A.; Schaad, L. J.; Henderson, D. O.; Fontana, L. P.; Smith, H. E.; Nafie, L. A.; Freedman, T. B.; Zuk, W. M. *J. Chem. Phys.* **1987**, *86*, 1140-1146.
(8) Freedman, T. B.; Paterlini, M. G.; Lee, N. S.; Nafie, L. A.; Schwab, J. M.; Ray, T. *J. Am. Chem. Soc.* **1987**, *109*, 4727-4728.
(9) Spencer, K. M.; Freedman, T. B.; Nafie, L. A., personal communication.
(10) Jalkanen, K. J.; Stephens, P. J.; Amos, R. D.; Handy, N. C. *J. Am. Chem. Soc.* **1988**, *110*, 2012-2013.
(11) Dutler, R. A Theoretical Study of Asymmetric Reactions Induced by Circularly Polarized Light—The Electrocyclic Interconversion of Deuterated Cyclobutenes and Butadienes. Ph.D. Thesis, University of Calgary, 1988.
(12) Cant, N. W.; Armstead, W. J. *Spectrochim. Acta, Part A* **1975**, *31A*, 839-853.
(13) Bertie, J. E.; Jacobs, S. M. *J. Chem. Phys.* **1978**, *68*, 97-101.
(14) (a) Nakanaga, T. *J. Chem. Phys.* **1980**, *73*, 5451-5458. (b) Nakanaga, T. *J. Chem. Phys.* **1981**, *74*, 5384-5392.
(15) Komornicki, A.; Pauzat, F.; Ellinger, Y. *J. Phys. Chem.* **1983**, *87*, 3847-3857.
(16) Hess, B. A.; Schaad, L. J.; Polavarapu, P. L. *J. Am. Chem. Soc.* **1984**, *106*, 4349-4352.
(17) Lowe, M.; Alper, J. S.; Kawiecki, R.; Stephens, P. J. *J. Phys. Chem.* **1986**, *90*, 41-50.
(18) Simandiras, E. D.; Amos, R. D.; Handy, N. C.; Lee, T. J.; Rice, J. E.; Remington, R. B.; Schaefer III, H. F. *J. Am. Chem. Soc.* **1988**, *110*, 1388-1393.
(19) Holzwarth, G.; Chabay, I. *J. Chem. Phys.* **1972**, *57*, 1632-1635.
(20) Schellman, J. A. *J. Chem. Phys.* **1973**, *58*, 2882-2886.
(21) Abbate, S.; Laux, L.; Overend, J.; Moscowitz, A. *J. Chem. Phys.* **1981**, *75*, 3161-3164.
(22) Abbate, S.; Laux, L.; Pultz, V.; Havel, H. A.; Overend, J.; Moscowitz, A. *Chem. Phys. Lett.* **1985**, *113*, 202-206.
(23) Escribano, J. R.; Freedman, T. B.; Nafie, L. A. *J. Phys. Chem.* **1987**, *91*, 46-49.
(24) Polavarapu, P. L. *Mol. Phys.* **1983**, *49*, 645-650.
(25) Barnett, C. J.; Drake, A. F.; Kuroda, R.; Mason, S. F. *Mol. Phys.* **1980**, *41*, 455-468.
(26) (a) Nafie, L. A.; Walnut, T. H. *Chem. Phys. Lett.* **1977**, *49*, 441-446. (b) Walnut, T. H.; Nafie, L. A. *J. Chem. Phys.* **1977**, *67*, 1491-1500. (c) Walnut, T. H.; Nafie, L. A. *J. Chem. Phys.* **1977**, *67*, 1501-1510.
(27) Nafie, L. A.; Polavarapu, P. L. *J. Chem. Phys.* **1981**, *75*, 2935-2944.
(28) (a) Freedman, T. B.; Nafie, L. A. *J. Chem. Phys.* **1983**, *78*, 27-31. (b) Freedman, T. B.; Nafie, L. A. *J. Chem. Phys.* **1983**, *79*, 1104.
(29) Nafie, L. A.; Freedman, T. B. *J. Chem. Phys.* **1983**, *78*, 7108-7116.
(30) (a) Stephens, P. J. *J. Phys. Chem.* **1985**, *89*, 748-752. (b) Stephens, P. J. *J. Phys. Chem.* **1987**, *91*, 1712-1715.
(31) Craig, D. P.; Thirunamachandran, T. *Mol. Phys.* **1978**, *35*, 825-840.

0002-7863/89/1511-6957$01.50/0 © 1989 American Chemical Society

intensities of a transition g → e are expressed in terms of the dipole strength $D_{g,e}$ and the rotational strength $R_{g,e}$ and are formally given by

$$D_{g,e} = \{\vec{\mu}_{g,e}\cdot\vec{\mu}_{e,g}\} = \{\langle\Phi_g|\vec{\mu}_{el}|\Phi_e\rangle\cdot\langle\Phi_e|\vec{\mu}_{el}|\phi_g\rangle\} = \frac{3(2303)hc}{8\pi^3 N_0}\int_{band}\frac{\epsilon(\nu)\,d\nu}{\nu} \quad (1)$$

$$R_{g,e} = \mathrm{Im}\,\{\vec{\mu}_{g,e}\cdot\vec{m}_{e,g}\} = \mathrm{Im}\,\{\langle\Phi_g|\vec{\mu}_{el}|\Phi_e\rangle\cdot\langle\Phi_e|\vec{\mu}_{mag}|\Phi_g\rangle\} = \frac{3(2303)hc}{32\pi^3 N_0}\int_{band}\frac{\Delta\epsilon(\nu)\,d\nu}{\nu} \quad (2)$$

Φ_g and Φ_e stand for the total molecular wave function of the ground state, g, and a particular vibrationally excited state, e, of the species. Both Φ_g and Φ_e contain a nuclear part describing the vibrational motion of the nuclei as well as an electronic part characterizing the electron–electron and electron–nucleus interactions in the molecule. The symbols h, c, N_0, and ν denote Planck's constant, the velocity of light, Avogadro's number, and the absorption frequency in cgs units, respectively. The operators $\vec{\mu}_{el}$ and $\vec{\mu}_{mag}$ represent the perturbation due to the electric and magnetic fields of the incident radiation and are formally given by

$$\vec{\mu}_{el} = \vec{m}^{n}_{el} + \vec{\mu}^{e}_{el} = \sum_{n=1}^{n_{atoms}}\xi_n\vec{r}_n + \sum_{i=1}^{n_{electrons}}\xi_i\vec{r}_i \quad (3)$$

$$\vec{\mu}_{mag} = \vec{\mu}^{n}_{mag} + \vec{\mu}^{e}_{mag} = \sum_{n=1}^{n_{atoms}}\frac{\xi_n}{2m_nc}(\vec{r}_n\times\vec{p}_n) + \sum_{i=1}^{n_{electrons}}\frac{\xi_i}{2m_ic}(\vec{r}_i\times\vec{p}_i) \quad (4)$$

where $\vec{\mu}^{n}_{el}$, $\vec{\mu}^{e}_{el}$, $\vec{\mu}^{n}_{mag}$, and $\vec{\mu}^{e}_{mag}$ denote the nuclear and electronic contributions of the electric and magnetic dipole transition moment operators, respectively. ξ_k symbolizes the charge of particle k, i.e., nucleus or electron with mass m_k that is located at a distance $\vec{r}_k$ from the physical origin of the system and is moving with a linear momentum of $\vec{p}_k$. $\vec{\mu}_{mag}$ is a Hermitian, purely imaginary operator, and hence Im, i.e., the imaginary part of the scalar product (2) ensures a real, measurable quantity R. While the commonly employed approach of substituting Born–Oppenheimer wave functions for the total molecular wave functions Φ works well for the evaluation of the electric dipole transition matrix elements $\langle\Phi_g|\vec{\mu}_{el}|\Phi_e\rangle$, the electronic part of the magnetic dipole transition moment elements $\langle\Phi_g|\vec{\mu}_{mag}|\Phi\rangle$ for vibrational transitions has been shown to vanish within the Born–Oppenheimer approximation.[29,32,33] It has thus been necessary to adopt more or less accurate approximation schemes to deal with this difficulty. Simple models that treat the nuclear motions explicitly but deal with the associated electronic rearrangements of charge only implicitly may restore some of the electronic contributions to the magnetic dipole transition moment. However, these methods are based on effective moment operators rather than their rigorous analogues. More meticulous treatments of the breakdown of the Born–Oppenheimer approximation make use of more accurate, non-Born–Oppenheimer wave functions to express the magnetic (and electric) transition moments of the molecule.

Infrared absorption intensities of the parent oxirane and oxirane-d_4 molecule have been measured by Nakanaga[14] and calculated by Lowe, Alper, Kawiecki, and Stephens (LAKS).[17] However, vibrational circular dichroism results are limited to modes of (*S*,*S*)-2,3-dideuteriooxirane above approximately 960 cm^{-1}.[8-10] The CH and CD stretching region has been the subject of investigation by the ab initio VCD formalism of Stephens and co-workers,[30] who achieved very good agreement with the features of the experimental spectrum.

In this paper, we present computational results from an ab initio implementation of the vibronic coupling theory of Nafie and Freedman[29] on the infrared absorption and vibrational circular dichroism intensities associated with the 15 fundamental, harmonic normal vibrations of the parent oxirane molecule, (*S*)-2-deuteriooxirane, (*S*,*S*)-2,3-dideuteriooxirane, (*S*,*R*)-2,3-dideuteriooxirane, 2,2-dideuteriooxirane, (*S*)-2,2,3-trideuteriooxirane, and 2,2,3,3-tetradeuteriooxirane. While infrared absorption intensities of these species can be rigorously evaluated with the atomic polar tensor approach,[34] vibrational circular dichroism requires a more sophisticated treatment. This article is divided into several sections: The theoretical background for infrared absorption and vibrational circular dichroism calculations is briefly reviewed; the computational details as employed throughout this work are discussed. The effects on the calculated intensities of variations in the initial molecular geometries, harmonic ab initio vibrational force constants, and basis sets are examined, while at the same time a quantitative comparison with experimental results of oxirane and oxirane-d_4 is attempted. Finally, the comparison of infrared absorption and vibrational circular dichroism intensities of all the above isotopomers of oxirane and if applicable also with experimentally accessible data is presented.

Theoretical Background

Both infrared absorption and vibrational circular dichroism owe their origin to a vibrational transition between stationary energy states of the molecule. The change from an initial state to another is promoted by the actions of the external oscillating electric and magnetic fields of the incident radiation, which causes, to a first approximation, changes in the nuclear vibrations in the molecule. In principle, the intensities can thus be expressed in terms of energy second derivatives with respect to the appropriate fields, $\vec{\mathcal{F}}$, and nuclear coordinates, $\vec{R}$, and hence belong to the class of second-order, nonlinear properties. Conceptually, it is straightforward to apply the Hellmann–Feynman theorem[35] to the evaluation of the energy derivatives with respect to the electric or magnetic fields, as the wave functions used in the computational process generally do not depend on the external fields. On the other hand, it is fundamentally wrong to apply the same procedure, i.e., the Hellmann–Feynman theorem to calculate derivatives with respect to nuclear coordinates as the wave functions employed are direct functions of the atomic positions. Nonetheless, as demonstrated shortly, in some cases it is possible to make provisions within the wave function so that inaccuracies approximately cancel and a pseudo-Hellmann–Feynman approach can be employed.

Assuming the validity of the Hellmann–Feynman theorem leads directly to the infrared and vibrational circular dichroism intensity expressions (1) and (2). However, calculated magnetic dipole transition moment elements unrealistically, i.e., unphysically, become zero within the Born–Oppenheimer approximation, necessitating the introduction of more or less approximate intensity emulation. Two of these models, namely, the atomic polar tensor (APT) and the vibronic coupling approaches, are used throughout this work and are thus treated in some detail below.

The ultimate expressions for infrared absorption intensities have been derived by Person and Newton[34] and are well-known, while the analogous atomic polar tensor expression for vibrational circular dichroism has only recently been presented in detail by Nafie and Freedman.[28] Within the premise of the APT formalisms, the electric and magnetic dipole transition moments are given by

$$\vec{\mu}^{APT}_{(00,01)_j} = \left(\frac{\hbar}{2\omega_j}\right)^{1/2}\sum_{n=1}^{n_{atoms}}\left(\frac{\partial\vec{\mu}}{\partial\vec{R}_n}\right)_0\vec{s}^{\,j}_n \quad (5)$$

$$\vec{m}^{APT}_{(01,00)_j} = \frac{i}{2c}\left(\frac{\hbar\omega_j}{2}\right)^{1/2}\sum_{n=1}^{n_{atoms}}\left[\vec{R}_{n,0}\times\left(\frac{\partial\vec{\mu}}{\partial\vec{r}_n}\right)_0\right]\cdot\vec{s}^{\,j}_n \quad (6)$$

where the subscripts (00,01) and (01,00) denote transitions between the zeroth and the first vibrational levels of the ground electronic state. The symbol ω_j refers to the vibrational frequency

(32) Mead, C. A.; Moscowitz, A. *Int. J. Quantum Chem.* **1967**, *1*, 243–249.
(33) Cohan, N. V.; Hameka, H. F. *J. Chem. Phys.* **1966**, *45*, 4392–4399.
(34) Person, W. B.; Newton, J. H. *J. Chem. Phys.* **1974**, *61*, 1040–1049.
(35) Feynman, R. P. *Phys. Rev.* **1939**, *56*, 340–343.

of the jth fundamental normal vibrations of all the atoms n that are on average located at position $\vec{R}_{n,0}$ and undergo a relative displacement $\vec{s}_n^j$. The components of the derivatives of the permanent dipole moments of the molecule with respect to nuclear displacement coordinates $(\partial\vec{\mu}/\partial\vec{R}_n)$ are the elements of a third-rank tensor that gives the name to this particular intensity model. While the above equation for the electric dipole transition moment is rigorous within the framework of the Hellmann–Feynman theory, the equivalent expression for the magnetic dipole transition moment is obtained in a semi-quantum mechanical procedure, which, however, does not repose on empirical quantities such as atomic charges, charge flux parameters, etc. Nonetheless, so as to retain a simple physical picture of vibrating, anisotropic charges that contribute to the absorption intensities, most crucial in the derivation of the APT model for vibrational circular dichroism is the assumption that an electron is associated with a particular nucleus. Hence, it is expected that strongly delocalized electrons and electronic motions induced distant from the vibrating nucleus bring about significant errors in this model.

On the basis of first principles, Nafie and Freedman also reported a rigorous approach that accounts for the missing velocity correlation in the Born–Oppenheimer approximation by means of standard Rayleigh–Schrödinger perturbation theory.[29] The final adiabatic contributions to the transition moments are derived as

$$\vec{\mu}^{VC}_{(00,01)_j} = \left(\frac{\hbar}{2\omega_j}\right)^{1/2}\left[\sum_{n=1}^{n_{atoms}} \xi_n \vec{s}_n^j - 2\sum_{n=1}^{n_{atoms}}\sum_{i=1}^{n_{electron}}\sum_{e=1}^{n_{ex}} \langle\Psi_0^a|\vec{r}_i|\Psi_e^a\rangle\left\langle\Psi_e^a\left|\frac{\partial}{\partial\vec{R}_n}\right|\Psi_0^a\right\rangle\vec{s}_n^j\right] \quad (7)$$

$$= \left(\frac{\hbar}{2\omega_j}\right)^{1/2}\left[\sum_{n=1}^{n_{atoms}} \xi_n \vec{s}_n^j - 2\sum_{n=1}^{n_{atoms}}\sum_{i=1}^{n_{electron}}\left\langle\Psi_0^a|\vec{r}_i\frac{\partial}{\partial\vec{R}_n}\right|\Psi_0^a\right\rangle\vec{s}_n^j\right] \quad (8)$$

$$\vec{m}^{VC}_{(01,00)_j} = \frac{1}{2c}\left(\frac{\hbar\omega_j}{2}\right)^{1/2}\left[i\sum_{n=1}^{n_{atoms}} \xi_n(\vec{R}_n \times \vec{s}_n^j) - \frac{2\hbar}{m_{electron}} \times \sum_{n=1}^{n_{atoms}}\sum_{i=1}^{n_{electron}}\sum_{e=1}^{n_{ex}} (\Psi_0^a|\vec{r}_i \times \vec{p}_i|\Psi_e^a)\left\langle\Psi_e^a\left|\frac{\partial}{\partial\vec{R}_n}\right|\Psi_0^a\right\rangle\vec{s}_n^j\frac{1}{E_e^0 - E_g^0}\right] \quad (9)$$

where Ψ_0^a and Ψ_e^a represent the total adiabatic wave function of the ground and excited electronic states of the molecule, respectively. Note that the electric dipole transition moments $\vec{\mu}^{APT}_{(00,01)_j}$ and $\vec{\mu}^{VC}_{(00,01)_j}$ are formally equivalent. The real and Hermitian form of the position operator $\vec{r}$ allows $\vec{\mu}^{VC}_{(00,01)_j}$ to be written in a closed form that does not involve a summation over excited states. Contrariwise, the operator $(\vec{r}_i \times \vec{p}_i)$ is a Hemitian, purely imaginary operator that is antisymmetric upon interchange of the wave functions. Thus, $\vec{m}^{VC}_{(01,00)_j}$ cannot be expressed in a closed form as the factor $1/(E_e^0 - E_g^0)$ prevents the summation over excited states from being carried out by means of the closure relation. However, Stephens proposed that the summation over excited states may be circumvented by introducing the derivative of the wave function with respect to the magnetic field.[30] The explicit summation over states is limited in practice by two considerations. Use of a finite basis set limits the number and kinds of states available for the sum, and the sum must be truncated for reasons of practicality. Rotational strengths (eq 2) obtained by using eq 9 are thus expected to be origin dependent.[36] We demonstrate by argument below and by numerical example further on that the truncated sum need not incur serious deleterious consequences, i.e., that the sum over states can be made "complete" in the sense that eq 7 and 8 are equivalent and that errors due to origin dependence are not severe.

The electronic wave functions Ψ, in eq 7–9, are constructed from molecular orbitals ψ_i in the form of Slater determinants. The molecular orbital functions ψ_i themselves are expressed as linear combinations of spatial basis functions $\{\phi\}$ such that

$$\Psi_i = \sum_{a=1}^{n_{atoms}}\sum_{\mu=1}^{n_{basis}{}^a} c_{\mu i}\phi_\mu^a \quad (10)$$

In turn, the atom-centered functions ϕ_μ^a are taken to be predefined linear combinations of Gaussian type orbitals (GTO):[37,38]

$$\phi_\mu^a = \sum_{j=1}^{n_{Gaussian}} d_{j\mu}\chi_j^a \quad (11)$$

where the primitive Gaussian functions χ_j^a are of the general form

$$\chi_j^a = N_j(x - x_a)^{l_{xj}}(y - y_a)^{l_{yj}}(z - z_a)^{l_{zj}}e^{-\alpha_j((x-x_a)^2+(y-y_a)^2+(z-z_a)^2)} \quad (12)$$

N_j represents a normalization constant, $l_{x,j}$, $l_{y,j}$, and $l_{z,j}$ define the symmetry property, that is, the angular quantum number of the function, and the exponent α_j is a measure of the radial expansion (tightness) of the function. The operators $\vec{r}_i$ and $(\vec{r}_i \times \vec{p}_i)$ are one-electron operators and yield nonzero matrix elements between determinants that differ in no more than two molecular orbitals or equivalently by a single-electron excitation. If the electronic part of the ground-state wave function is the Hartree–Fock determinant, only the singly excited configurations that appear in the expansion of the excited states will yield nonzero transition matrix elements and need be considered in the sum to first order. Thus, the sum over excited states consists of all singly excited singlet configurations, and the energy difference $(E_e - E_g)$ is evaluated by taking into account the Coulomb and exchange integrals over the orbitals involved in each excited configuration.

The operator $(\partial/\partial\vec{R}_n)$ behaves the same way as a one-electron operator in that transition matrix elements connect only single excited configurations to the Hartree–Fock determinant. Consequently, the sum over states reduces to sums over occupied and unoccupied molecular orbitals, ψ_i and ψ_a, respectively, appearing in matrix elements of the form $(\psi_a|\partial/\partial\vec{R}_n|\psi_i)$. "Completeness" of the sum over states translates into the ability to express the derivative of an occupied MO as a linear combination of the Hartree–Fock molecular orbitals:

$$\frac{\partial\psi_i}{\partial\vec{R}} \approx \sum_j^{n_{basis}} a_j\psi_j \quad (13)$$

In principle, eq 5–9 may be evaluated in a straightfoward manner. However, the spatial derivatives of the form $\partial\Psi/\partial\vec{R}$ appearing in these equations are somewhat obstructive in the practical implementation of the transition moment expressions. From the form of the single Slater determinantal wave function Ψ together with eq 10, the derivatives involve terms such as $\partial c_{\mu i}/\partial\vec{R}$ and $\partial\phi_\mu/\partial\vec{R}$, the former of which are obtained by means of standard coupled perturbed Hartree–Fock theory.[39–43] As evident from the expansion (11), $\partial\phi_\mu/\partial\vec{R}$ produces a linear combination of functions of the type $\partial\chi_i/\partial\vec{R}$, which in view of eq 12 and carrying out the differentiation yield Gaussian functions that are multiplied by their own exponents. Consequently, in a fixed linear combination of primitive Gaussian functions defining a particular atomic orbital, the tighter functions gain in importance. Hence, parts of $\partial\phi_\mu/\partial\vec{R}$ may be outside the range of the original basis set $\{\phi\}$, which for this reason can only inadequately describe the derivatives $\partial\phi_\mu/\partial\vec{R}$.

(36) Moscowitz, A. *Modern Quantum Chemistry*; Sinanoglu O., Ed.; Academic Press: New York, 1965; Vol. III.

(37) Hehre, W. J.; Radom, L.; Schleyer, P. v. R.; Pople, J. A. *Ab Initio Molecular Orbital Theory*; Wiley: New York, 1986.

(38) Hurley, A. C. *Proc. R. Soc., London* **1954**, *A226*, 179–192.

(39) Pople, J. A.; Krishnan, R.; Schlegel, H. B.; Binkley, J. S. *Int. J. Quantum Chem. Symp.* **1979**, *13*, 225–241.

(40) (a) Gerratt, J.; Mills, I. M. *J. Chem. Phys.* **1968**, *49*, 1719–1729. (b) Gerratt, J.; Mills, I. M. *J. Chem. Phys.* **1968**, *49*, 1730–1739.

(41) Thomsen, K.; Swanstrøm, P. *Mol. Phys.* **1973**, *26*, 735–750.

(42) Takada, T.; Dupuis, M.; King, H. F. *J. Chem. Phys.* **1981**, *75*, 332–336.

(43) Almlöf, J.; Taylor, P. R. *Int. J. Quantum Chem.* **1985**, *27*, 743–768.

With use of the above considerations, the quality of the electronic wave function Ψ with respect to its applicability in the Hellmann–Feynman theorem for geometric derivatives may be assessed by writing the spatial derivative of one particular molecular orbital ψ_i as a linear combination of all the molecular orbitals in the set which for practical applications contains a finite number, n_{basis}, of functions (13). In the limit of a complete set $\{\psi\}$ the left- and right-hand sides of eq 13 are equal. For an incomplete set of functions, however, this condition is only approximately fulfilled, but the situation may be significant improved by including first-order derivative functions into the original basis set.[11,44-48] The geometric derivative of an atomic orbital, ϕ_μ^l, originating from differentiating the linear combinations of AOs, defining a particular molecular orbital yields, with the exception of s-type AOs two type of functions, $\tilde{\phi}'^{(l+1)}_\mu$ and $\tilde{\phi}^{(l-1)}_\mu$, corresponding to an increase and decrease in the angular momentum quantum number l by one. Hence

$$\frac{\partial \phi_\mu^l}{\partial \bar{R}} = \tilde{\phi}'^{(l+1)}_\mu + [\tilde{\phi}^{(l-1)}_\mu]_{l\neq 0} \quad (14)$$

The functions $\tilde{\phi}'$ on the right-hand side of the above expression have radial and angular properties much the same as the atomic orbitals ϕ. Introducing a normalization factor, $N_\mu^{(l\pm1)}$, the functions $\phi'^{(l\pm1)}_\mu$ can be written in terms of properly normalized atomic orbitals $\phi_\mu^{(l\pm1)}$:

$$\tilde{\phi}'^{(l\pm1)}_\mu = N_\mu^{(l\pm1)} \tilde{\phi}_\mu^{(l\pm1)} \quad (15)$$

The left-hand side of this equation originates from the derivative of the atomic orbitals ϕ_μ^l and therefore also involves an expansion in terms of GTOs, $\tilde{\chi}_i^{(l\pm1)}$, that are the single Gaussian analogues of $\tilde{\phi}'^{(l\pm1)}_i$. The function $\tilde{\chi}_i^{(l\pm1)}$ on the right-hand side can be expressed in terms of primitive, normalized Gaussian functions, and thus the above equation becomes

$$\sum_i d_{i\mu}^l \tilde{\chi}'^{(l\pm1)}_i = N_{i\mu}^{(l\pm1)} \tilde{\chi}_j^{(l\pm1)} \quad (16)$$

Evaluating the derivative of a Gaussian type function does not alter its tightness, i.e., the exponent α of the function. Thus, it appears reasonable to assume that there is a one to one correspondence between the derivative, $\tilde{\chi}'^{(l\pm1)}_i$ and the "fitting" function $\tilde{\chi}_i^{(l\pm1)}$. This implication allows a term by term separation of the above equation such that

$$d_{i\mu}^l \tilde{\chi}'^{(l\pm1)}_i(\alpha_i) = N_\mu^{(l\pm1)} \tilde{d}_{i\mu}^{(l\pm1)} \tilde{\chi}_i^{(l\pm1)}(\alpha_i) \quad (17)$$

With this relation, in conjunction with the particular form of the Gaussian functions (12), it is a facile process to demonstrate that the contraction coefficients $\tilde{d}_{i\mu}^l$ of the new atomic orbital $\tilde{\phi}_{i\mu}^{(l\pm1)}$ are directly related to the original set $d_{i\mu}^l$ by

$$\frac{\tilde{d}_{i\mu}^{(l\pm1)}}{d_{i\mu}^l} = \frac{\langle \tilde{\chi}_i^{(l\pm1)}(\alpha_i) | \tilde{\chi}'^{(l\pm1)}_i(\alpha_i) \rangle}{N_\mu^{(l\pm1)}} = \frac{(\alpha_i)^{1/2}}{N_\mu^{(l\pm1)}} \quad (18)$$

This important result may then be interpreted as follows: Although the initial basis set is incomplete for an application within the premise of the Hellmann–Feynman theorem, additional functions may be tailored and added to the original set so as to improve the mathematical description. For each atomic orbital in the beginning set, two new types of basis functions need to be introduced according to a change in the angular momentum quantum number of plus or minus one. The original and the new functions are both made up of the same number of primitive Gaussians with identical exponents but different contraction coefficients. The new contraction coefficients are related to the original set by the square root of the appropriate Gaussian exponent and subsequent renormalization of the resulting atomic orbital.

Unfortunately, the above procedure is not a complete solution as the inclusion of the derivative functions, $\tilde{\phi}_\mu^{(l\pm1)}$, also requires functions that describe their derivatives, and so on, ad infinitum. Nakatsuji et al. have shown, however, that the inclusion of the first derivatives $\tilde{\phi}_\mu^{(l\pm1)}$ causes the basis to obey the Hellmann–Feynman theorem to first order.[48]

Reliable predictions of calculated intensities go hand in hand with accurate determinations of the force field, vibrational frequencies, and normal modes. As a general rule, vibrational frequencies on the Hartree–Fock level of theory are calculated to be approximately 5–10% higher than experimental, harmonic values.[49,50] This is primarily due to the overestimation of diagonal force constants that arises because of a too-steep potential function predicted by Hartree–Fock, single Slater determinantal wave function. These errors are quite systematic. In some cases it is thus feasible to adjust the frequencies by a simple multiplication with a constant factor.[51,52] Better agreement may be obtained, however, by limited nonuniform scaling of the stretching, bending, or torsional force constants associated with the vibrational motions of the different groups in the molecule.[5,50,53,54] In this procedure, the force constants are scaled such that

$$F_{ij}^{scaled} = (c_i c_j)^{1/2} F_{ij}^{calc} \quad (19)$$

We describe below the results of several levels of scaling, basis set, and geometry on oxirane and oxirane-d_4 with particular emphasis on the quality of the infrared absorption intensities as compared to experimental values.

Computational Details

For the purpose of determining the importance of a suitable molecular structure and basis set for harmonic frequency analyses, infrared absorption, and vibrational circular dichroism intensities of oxirane and several of its deuterated analogues, three sets of geometries have been employed in conjunction with the 6-31g**[57] basis set, as well as the 6-31g[60] basis augmented by a truncated set of first-order derivative functions, henceforth denoted by a tilde (~). The geometries correspond to the experimental microwave structure of oxirane determined by Hirose,[61] as well as the two geometries of oxirane obtained by full, analytical gradient optimizations[55] within the constraints of RHF theory[56] employing the basis sets above and the GAUSSIAN82 system of programs.[58] The 6-31g** basis set is an energy optimized basis that provides the molecule orbital calculations with a high degree of flexibility through the usage of diffuse d functions on oxygen and carbon and p functions on hydrogen. The derivatived basis set, designated 6-31g̃(-2s̃,2p̃,2p̃$_H$), is derived from the standard 6-31g basis, by addition of all first-order spatial derivatives with the exception of the inner 2s$_{C,O}$, 2s$_H$, and the s component of the inner 2p$_{C,O}$ basis functions, namely, 2p̃, 2p̃$_H$, and 2s̃, respectively. These last have been shown to be insignificant for infrared absorption and

(44) Sadlej, A. J. *Chem. Phys. Lett.* **1977**, *47*, 50–54.
(45) Roos, B. O.; Sadlej, A. J. *Chem. Phys.* **1985**, *94*, 43–53.
(46) Wolinski, K.; Roos, B. O.; Sadlej, A. J. *Theoret. Chim. Acta* **1985**, *68*, 431–444.
(47) Lazzaretti, P.; Zanasi, R.; Fowler, P. W. *J. Chem. Phys.* **1988**, *88*, 272–276.
(48) Nakatsuji, H.; Kanda, K.; Yonezawa, T. *Chem. Phys. Lett.* **1980**, *75*, 340–346.
(49) Pulay, P.; Lee, J. G.; Boggs, J. E. *J. Chem. Phys.* **1983**, *79*, 3382–3391.
(50) Pulay, P. In *Modern Theoretical Chemistry*; Schaefer III, H. F., Ed.; Plenum Press: New York, 1977; Vol. 4.
(51) Pople, J. A.; Schlegel, H. B.; Krishnan, R.; DeFrees, D. J.; Binkley, J. S.; Frisch, M. J.; Whiteside, R. A.; Hout, R. F.; Hehre, W. J. *Int. J. Quantum Chem. Symp.* **1981**, *15*, 269–278.
(52) Hout, R. F.; Levi, B. A.; Hehre, W. J. *J. Comput. Chem.* **1982**, *3*, 234–250.
(53) Blom, C. E.; Altona, C. *Mol. Phys.* **1976**, *31*, 1377–1391.
(54) Shaw, R. A.; Ursenbach, C.; Rauk, A.; Wieser, H. *Can. J. Chem.* **1988**, *66*, 1318–1332.
(55) Schlegel, H. B. *J. Comput. Chem.* **1982**, *3*, 214–218.
(56) Roothan, C. C. J. *Rev. Mod. Phys.* **1951**, *23*, 69–89.
(57) Hehre, W. J.; Ditchfield, R.; Pople, J. A. *J. Chem. Phys.* **1972**, *56*, 2257–2261.
(58) Binkley, J. S.; Frisch, M. J.; DeFrees, D. J.; Raghavachari, K.; Whiteside, R. A.; Schlegel, H. B.; Fluder, E. M.; Pople, J. A. Department of Chemistry, Carnegie-Mellon University, Pittsburgh, PA.
(59) Møller, C.; Plesset, M. S. *Phys. Rev.* **1934**, *46*, 618–622.
(60) (a) Binkley, J. S.; Pople, J. A. *J. Chem. Phys.* **1977**, *66*, 879–880. (b) Francl, M. M.; Pietro, W. J.; Hehre, W. J.; Binkley, J. S.; Gordon, M. S.; DeFrees, D. J.; Pople, J. A. *J. Chem. Phys.* **1982**, *77*, 3654–3665.
(61) Hirose, C. *Bull. Chem. Soc. Jpn.* **1974**, *47*, 1311–1318.

Table I. Molecular Geometries (in angstroms and degrees) and RHF Energies (in hartrees) of Oxirane

geom	basis set	r_{CO}	r_{CC}	r_{CH}	∠HCH	τ_{HCCO}	E(RHF)
expt[a]	6-31g**	1.434	1.470	1.085	116.3	103.3	-152.872 378
	6-31g̃(-2s̃,2p̃,2p̃$_H$)						-152.861 324
6-31g**	6-31g**	1.401	1.453	1.078	115.2	103.2	-152.874 065
	6-31g̃(-2s̃,2p̃,2p̃$_H$)						-152.861 776
6-31g̃(-2s̃,2p̃,2p̃$_H$)	6-31g̃(-2s̃,2p̃,2p̃$_H$)	1.419	1.455	1.073	115.4	103.1	-152.862 182

[a] Experimental geometry determined by Hirose.[61]

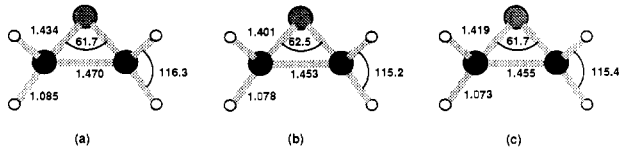

Figure 1. Experimental (a), 6-31g** (b), and 6-31g̃(-2s̃,2p̃,2p̃$_H$) (c) geometries of parent oxirane molecule.

vibrational circular dichroism intensity type of applications.[11] The 6-31g̃(-2s̃,2p̃,2p̃$_H$) basis set differs from the 6-31g** set in that it contains two sets of d functions and an additional set of p functions on carbon and oxygen. Furthermore, generally the derivative functions of the 6-31g̃(-2s̃,2p̃,2p̃$_H$) basis set are more compact than the diffuse polarization functions in the 6-31g** basis set.

In this work, harmonic vibrational force fields have been calculated by using analytical second energy derivative techniques[39-43] as implemented in the GAUSSIAN82 molecular orbital programs. Solution of the CPHF equations yields the geometric derivatives of the molecular orbital coefficients, $\partial c_{\mu i}/\partial \vec{R}$. Vibrational frequencies, and normal coordinates $\vec{s}_n^i$ were obtained by standard methods[62-64] utilizing the above ab initio force constants as well as with uniformly and nonuniformly scaled force constants as advocated by Pulay et al.[49,50] and implemented by Shaw.[5,54] Infrared absorption and vibrational circular dichroism intensities have been evaluated by means of eq 5, 6 and 8, 9, that is, by employing Nafie and Freedman's atomic polar tensor (APT) and vibronic coupling (VC) descriptions for vibrational intensities, which are coded in the FREQ85 program running on a CDC CYBER205 supercomputer.[11,65] All moments are evaluated at a common origin, the molecular center of mass. Origin dependence of the rotatory strength is tested by explicit recalculation of the VCD results for (*S*,*S*)-2,3-dideuteriooxirane at an origin (0.5 Å, 0.5 Å, 0.5 Å) relative to the molecular center of mass. Infrared and vibrational circular dichroism spectra are simulated by assuming Lorentzian line shapes of the bands with a constant half-width of 10 cm^{-1}. Results of the computations involving the three different starting geometries, unscaled and scaled force fields, and the APT and VC intensity models are presented and discussed in the following.

Results and Discussion

Geometries. The equilibrium geometries for oxirane obtained with the 6-31g** and 6-31g̃(-2s̃,2p̃,2p̃$_H$) basis sets are presented in Table I in conjunction with Figure 1, together with the experimental geometry. The two basis sets yield very similar geometries. The major different appears in the C–O bond distance, which is calculated to be 0.018 Å longer with the latter. Both basis sets yield bonds that are shorter than observed,[17] although slightly better disagreement is obtained with the 6-31g̃(-2s̃,2p̃,2p̃$_H$) basis set. The shorter bond lengths appear to be a feature of the SCF calculations since optimization with correlated wave functions have been reported to yield a geometry in closer agreement with experiment.[18]

Harmonic Vibrational Frequencies of Oxirane and Oxirane-d_4. Harmonic force constants were calculated at the 6-31g** and 6-31g̃(-2s̃,2p̃,2p̃$_H$) equilibrium geometries and at the experimental geometry by using both basis sets for oxirane and oxirane-d_4. 6-31g** frequencies at the 6-31g** equilibrium geometry are consistent with MP2 frequencies reported by Simandiras et al.[18] in that they suggest a possible reversal in the assignments of the experimental bands at 1120 and 1159 cm^{-1}. We note that 6-31g̃(-2s̃,2p̃,2p̃$_H$) results reproduce the experimental assignments of these two bands.[14] In the analysis described below, we assume that the experimental assignments are correct.

The raw, ab initio force constance were subjected to uniform scaling and to nonuniform scaling with three and seven scale factors to improve the agreement between calculated and observed frequencies. The observed data for oxirane and oxirane-d_4[14] were combined for the purpose of the least-squares fitting. Three scale factors were obtained by requiring that the C–H and C–C diagonal stretching constants be scaled by the same factor, the scale factor for the C–O stretch be allowed to vary independently, and all angle deformations be scaled by the same factor. The number of independent scale factors was increased to seven by relaxing the constraint on the C–H and C–C stretches and by scaling the internal wagging, twisting, rocking, and scissoring motions of the CH_2 groups independently. The results for selected tests are presented in Table II, together with the experimentally observed frequencies, arranged in ascending order for ease of comparison. The average discrepancy between calculated and observed values, expressed in cm^{-1} and as a percent, is also provided. Uniform scaling of the force constants derived at the experimental geometry by using either basis set (6-31g̃(-2s̃,2p̃,2p̃$_H$) is shown in Table II) yields the incorrect order of the lowest three normal modes. The correct order is obtained if either equilibrium geometry is used with either basis set (not all tests shown). Nonuniform scaling, of course, yields the correct order in every case. The closest agreement with experiment is observed with the force constants obtained with the 6-31g̃(-2s̃,2p̃,2p̃$_H$) basis set at the 6-31g̃(-2s̃,2p̃,2p̃$_H$) equilibrium geometry, scaled by seven parameters. However, the results are not substantially worse if only three scale factors are used and fall within acceptable limits even with uniform scaling, except where the experimental geometry is used.

Nonuniform scaling alters the normal modes from the ab initio values. It does not follow necessarily that improvement of the agreement with experiment with respect to frequencies would result in concomitant improvement in the normal modes of vibration expressed in terms of the Cartesian displacement vectors that appear in eq 5–9. IR and VCD intensities depend directly on these vectors.

IR Intensity Calculations. Basis Sets. Experimentally derived intensities are available for most of the fundamental modes of oxirane and oxirane-d_4.[14] These are cited in Table III, together with intensities calculated by using expressions 5 (=8) and 7. The required Cartesian displacement vectors were derived from a variety of sources, two of which are as indicated in Table III. It is clear from inspection of Table III that APT yields reasonable values for the IR intensities regardless of whether or not a "dervatized" basis set is used. The comparison (not shown) where the force field is nonuniformly scaled with seven factors (7sf) favors slightly the 6-31g̃(-2s̃,2p̃,2p̃$_H$) basis set, but the bias is not compelling.

Radically different values are obtained by use of the 6-31g** basis set and expression 7, which is formally equivalent to 8 and 5 but in which the sum over excited states is explictly carried out. A similar comparison in the case of the 6-31g̃(-2s̃,2p̃,2p̃$_H$) basis set reveals that 7 and 8 (=5) give very similar results, as expected on the basis of the arguments advanced above. This result is of

(62) Wilson, E. B., Jr.; Decius, J. C.; Cross, P. C. *Molecular Vibrations*; McGraw-Hill: New York, 1955.
(63) Steele, D. *Theory of Vibrational Spectroscopy*; W. B. Saunders: Toronto, 1971.
(64) Califano, S. *Vibrational States*; Wiley: Toronto, 1976.
(65) Dutler, R.; Rauk, A. Department of Chemistry, The University of Calgary, Calgary, Canada.

Table II. Harmonic Vibrational Frequencies (in cm^{-1}) of Oxirane and Its Tetradeuterated Analogue

basis set		6-31g** 6-31g**		6-31g̃(-2s̃,2p̃,2p̃$_H$) 6-31g̃(-2s̃,2p̃,2p̃$_H$)				6-31g̃(-2s̃,2p̃,2p̃$_H$) exptl[a]	
geom	exptl[b]	0sf	7sf[c]	0sf	1sf[d]	3sf[e]	7sf[e,f]	0sf	7sf[g]
				Oxirane					
ν_1 (B_1)	808	883	798	891	804	802	805	941	818
ν_2 (B_2)	822	975	822	927	836	825	823	888	824
ν_3 (A_1)	877	990	870	960	866	863	869	927	871
ν_4 (A_2)		1149	1028	1139	1027	1024	1026	1164	1001
ν_5 (A_1)	1120	1303	1145	1275	1151	1145	1138	1272	1138
ν_6 (B_1)	1147	1284	1159	1267	1143	1140	1153	1279	1148
ν_7 (B_2)	1159	1290	1146	1286	1160	1157	1147	1305	1145
ν_8 (A_2)		1285	1172	1288	1162	1159	1175	1309	1187
ν_9 (A_1)	1270	1423	1272	1401	1264	1264	1274	1375	1270
ν_{10} (B_2)	1470	1639	1461	1640	1479	1475	1468	1644	1469
ν_{11} (A_1)	1498	1694	1512	1684	1519	1516	1513	1681	1513
ν_{12} (B_2)	2978	3266	2990	3284	2963	2993	2988	3176	2987
ν_{13} (A_1)	3024	3279	3002	3296	2974	3004	3000	3187	2998
ν_{14} (A_2)		3351	3067	3372	3042	3073	3068	3265	3071
ν_{15} (B_1)	3065	3368	3083	3388	3057	3087	3083	3281	3085
				2,2,3,3-Tetradeuteriooxirane					
ν_1 (B_1)	577	630	569	635	573	571	574	670	585
ν_2 (A_2)		815	750	810	730	728	727	828	708
ν_3 (A_1)	752	830	737	824	743	742	743	817	746
ν_4 (B_2)	812	955	806	909	820	809	807	870	807
ν_5 (B_1)	898	1000	902	985	888	886	895	988	890
ν_6 (B_2)	900	1016	904	1012	913	910	902	1026	901
ν_7 (A_2)		1027	912	1027	927	924	940	1037	951
ν_8 (A_1)	968	1119	981	1095	988	981	977	1075	975
ν_9 (A_1)	1013	1140	1009	1115	1006	1005	1004	1111	1003
ν_{10} (B_2)	1083	1205	1073	1205	1087	1083	1078	1208	1080
ν_{11} (A_1)	1312	1485	1326	1453	1311	1312	1323	1416	1322
ν_{12} (B_2)	2177	2357	2158	2371	2139	2161	2158	2292	2156
ν_{13} (A_1)	2204	2398	2194	2409	2174	2195	2194	2327	2190
ν_{14} (A_2)		2504	2290	2520	2274	2296	2293	2442	2295
ν_{15} (B_1)	2322	2512	2300	2527	2280	2303	2299	2449	2302
av error			11.1 0.8%		14.6 0.9%	11.2 0.7%	9.4 0.6%		10.6 0.7%

[a] Microwave geometry by Hirose.[61] [b] Measured fundamental frequencies by Nakanaga et al.[14] [c] Scaling factors: 0.712 (CO stretch), 0.849 (CC stretch), 0.838 (CH stretch), 0.794 (scissor), 0.729 (rock), 0.789 (wag), 0.913 (twist). [d] Scaling factor: 0.814. [e] Scaling factor: 0.792 (CO stretch), 0.831 (CC and CH stretches), 0.809 (all angles). [f] Scaling factors: 0.789 (CO stretch), 0.867 (CC stretch), 0.828 (CH stretch), 0.801 (scissor), 0.852 (rock), 0.795 (wag), 0.792 (twist). [g] Scaling factors: 0.859 (CO stretch), 0.926 (CC stretch), 0.884 (CH stretch), 0.798 (scissor), 0.863 (rock), 0.771 (wag), 0.704 (twist).

no consequence for IR intensity calculations since one would use APT and avoid the sum over states. However, the result is of paramount importance for VCD intensity calculations since it is not possible to avoid the sum over excited states in evaluating the magnetic dipole transition moment, 9. For VCD calculations the use of the "derivatized" basis set is mandatory.

IR Intensity Calculations. Effect of Scaling the Force Field. Calculated IR intensities for oxirane and oxirane-d_4 by APT (5 or 8) from 6-31g̃(-2s̃,2p̃,2p̃$_H$) force fields at equilibrium and experimental geometries as a function of scaling are collected in Table IV. The experimental values are repeated, and the values of Lowe, Alper, Kawiecki, and Stphens (LAKS)[17] are included. Uniform scaling of the ab initio force constants does not affect the normal modes or the calculated intensities. Comparison of the intensities from uniform scaling (columns labeled 1sf in Table IV) with the experimental results shows reasonable agreement amongst the strongest bands. Judicious nonuniform scaling by three (3sf) or seven (7sf) scale factors does not result in as dramatic shifts in intensities as appears in the data of LAKS (oxirane bands ν_5 and ν_9; oxirane-d_4 bands ν_8-ν_{11}). Indeed, nonuniform scaling in most cases leads to a slight deterioration in the level of agreement with the experimental values. IR spectra obtained with the 6-31g̃(-2s̃,2p̃,2p̃$_H$) basis sets at the fully optimized geometry and subsequent nonuniform scaling of the ab initio force constants are schematically drawn in Figures 2 and 3.

Frequencies and IR Intensities for Other Deuterated Oxiranes. The predicted harmonic frequencies for 2-deuteriooxirane, *syn*- and *anti* 2,3-dideuteriooxirane, 2,2-dideuteriooxirane, and 2,2,3-trideuteriooxirane are given in Table V, in ascending order. The values result from uniform scaling of the ab initio values by the same scaling factor as obtained for oxirane and tetradeuteriooxirane, i.e., 0.814. The average error is expected to be approximately 15 cm^{-1} (0.9%). The corresponding IR intensities are presented in Table VI and also graphically displayed in Figures 4–8. The predicted frequencies and IR intensities in Table V and VI were obtained by using the 6-31g̃(-2s̃,2p̃,2p̃$_H$) basis set at the equilibrium geometry. The intensities were calculated by APT (5 or 8).

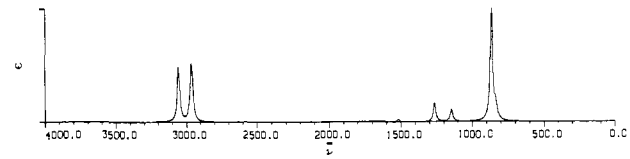

Figure 2. Relative 6-31g̃(-2s̃,2p̃,2p̃$_H$)/6-31g̃(-2s̃,2p̃,2p̃$_H$)/1sf infrared intensities of oxirane.

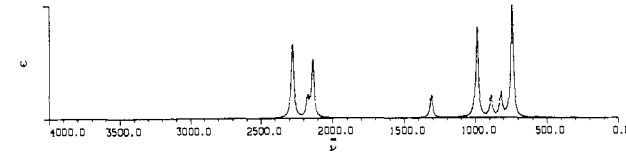

Figure 3. Relative 6-31g̃(-2s̃,2p̃,2p̃$_H$)/6-31g̃(-2s̃,2p̃,2p̃$_H$)/1sf infrared intensities of 2,2,3,3-tetradeuteriooxirane.

VCD Intensities for (*S*,*S*)-2,3-Dideuteriooxirane

The data and discussion presented above suggest that the most reliable prediction of VCD intensities is expected if one employs

Table III. APT vs Infrared SOS Intensities (in km/mol) of Oxirane and Oxirane-d_4 at Fully Optimized Geometry and Uniform Scaling[a]

	6-31g**		6-31g̃(−2s̃,2p̃,2p̃$_H$)		
basis set	APT[b]	SOS[c]	APT[b]	SOS[c]	exptl[d]
		Oxirane			
ν_1 (B_1)	0.0	8.4	0.5	0.5	0.21
ν_2 (B_2)	11.0	0.2	9.6	8.0	8.56
ν_3 (A_1)	83.7	105.8	81.7	82.2	63.94
ν_4 (A_2)	0.0	0.0	0.0	0.0	
ν_5 (A_1)	4.5	10.4	1.3	0.9	
ν_6 (B_1)	7.2	8.0	7.6	7.0	
ν_7 (B_2)	0.2	0.1	0.0	0.0	
ν_8 (A_2)	0.0	0.0	0.0	0.0	
ν_9 (A_1)	16.9	1.4	13.4	12.8	13.16
ν_{10} (B_2)	1.1	21.5	0.0	0.1	0.34
ν_{11} (A_1)	5.4	8.0	1.8	1.5	1.04
ν_{12} (B_2)	48.6	126.2	36.3	37.7	44.30
ν_{13} (A_1)	10.5	25.8	10.0	10.3	6.04
ν_{14} (A_2)	0.0	0.0	0.0	0.0	
ν_{15} (B_1)	66.0	211.8	39.8	44.0	36.24
		2,2,3,3-Tetradeuteriooxirane			
ν_1 (B_1)	0.0	17.6	0.3	0.3	0.45
ν_2 (A_2)	0.0	0.0	0.0	0.0	
ν_3 (A_1)	38.9	6.6	42.8	42.3	34.23
ν_4 (B_2)	9.2	2.8	8.9	7.3	6.76
ν_5 (B_1)	7.8	5.3	7.9	7.0	3.80
ν_6 (B_2)	0.0	3.4	0.1	0.0	0.10
ν_7 (A_2)	0.0	0.0	0.0	0.0	
ν_8 (A_1)	3.0	13.4	34.2	33.7	23.14
ν_9 (A_1)	40.8	104.8	1.3	1.1	1.69
ν_{10} (B_2)	1.8	48.1	0.2	0.1	0.05
ν_{11} (A_1)	16.6	7.2	8.6	7.6	6.43
ν_{12} (B_2)	29.4	121.8	21.9	23.0	19.89
ν_{13} (A_1)	8.4	23.9	7.0	7.1	7.17
ν_{14} (A_2)	0.0	0.0	0.0	0.0	
ν_{15} (B_1)	44.7	237.7	28.0	31.5	23.77

[a] Scaling factor: 0.814. [b] Atomic polar tensor model (eq 5, 8). [c] Vibronic coupling model, sum over excited states not closed (eq 7). [d] Experimental infrared absorption intensities, Nakanaga et al.[14]

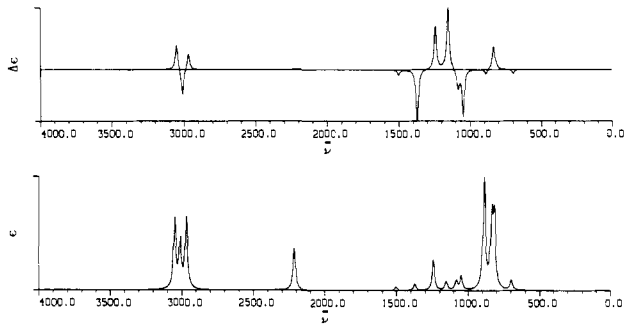

Figure 4. Relative to 6-31g̃(-2s̃,2p̃,2p̃$_H$)/6-31g̃(-2s̃,2p̃,2p̃$_H$)/1sf infrared and vibrational circular dichroism intensities of (*S*)-2-deuteriooxirane.

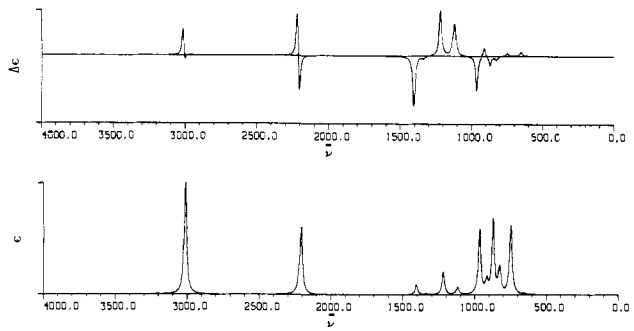

Figure 5. Relative 6-31g̃(-2s̃,2p̃,2p̃$_H$)/6-31g̃(-2s̃,2p̃,2p̃$_H$)/1sf infrared and vibrational circular dichroism intensities of (*S,S*)-2,3-dideuteriooxirane.

the 6-31g̃(-2s̃,2p̃,2p̃$_H$) basis set in a consistent manner (i.e., to obtain the geometry, frequencies, normal modes, and atomic polar tensors). Judicious nonuniform scaling does not result in substantial changes in the normal modes themselves, although such changes as do take place seem to be deleterious as judged by the quality of computed IR intensities. While experimental data are very sparse, we repeat in Table VII some of the tests of Tables III and IV on (*S,S*)-2,3-dideuteriooxirane to examine the effect of basis sets (6-31g** vs 6-31g̃(-2s̃,2p̃,2p̃$_H$)), level of scaling (uniform, 1sf vs nonuniform, 7sf), completeness of the basis set (eq 7 vs eq 8), theoretical model (APT, eq 5 and 6 vs VC, eq 8 and 9), and origin dependence (values in parentheses in last two columns). We expect that the most accurate results overall are in the second to last column, which employs the 6-31g̃(-2s̃,2p̃,2p̃$_H$) basis set, uniform scaling of the force constant matrix, vibronic coupling theory with eq 8 and 9 for the electric and magnetic dipole transition matrix elements, respectively, and moments evaluated at the center of mass. The results in this column serve as the reference point for the discussion below.

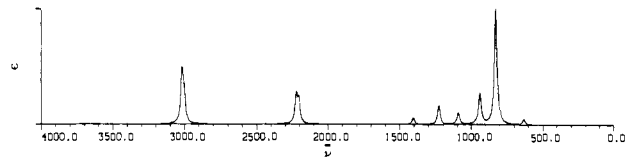

Figure 6. Relative 6-31g̃(-2s̃,2p̃,2p̃$_H$)/6-31g̃(-2s̃,2p̃,2p̃$_H$)/1sf infrared intensities of (*S,R*)-2,3-dideuteriooxirane.

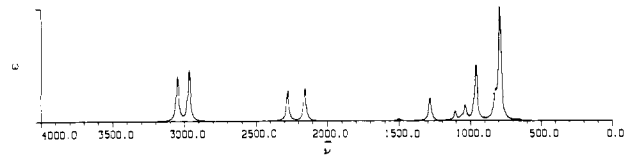

Figure 7. Relative 6-31g̃(-2s̃,2p̃,2p̃$_H$)/6-31g̃(-2s̃,2p̃,2p̃$_H$)/1sf infrared intensities of 2,2-dideuteriooxirane.

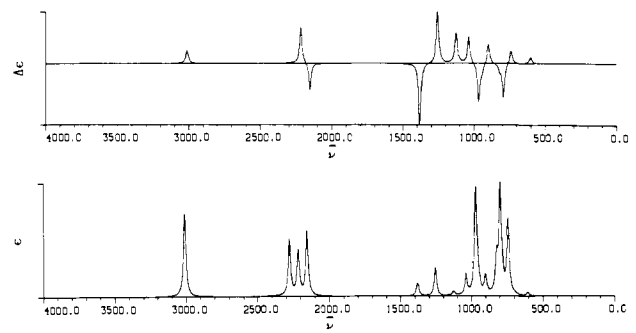

Figure 8. Relative 6-31g̃(−2s̃,2p̃,2p̃$_H$)/6-31g̃(-2s̃,2p̃,2p̃$_H$)/1sf infrared and vibrational circular dichroism intensities of (*S*)-2,2,3-trideuteriooxirane.

VCD. Completeness of Basis Set. Completeness, as discussed above, refers to the ability of the basis set to enable the generation of the correct excited-state wave functions so that truncation of the sum over states in eq 7 and especially eq 9 where it is unavoidable does not lead to serious errors. Comparison of the data in columns 7 and 8 and columns 10 and 11 reveals that the 6-31g̃(-2s̃,2p̃,2p̃$_H$) basis set satisfies the completeness criterion to an excellent extent with respect to VCD calculations. No pairs of numbers differ in sign of Cotton effect, and only two pairs (for band ν_{10}) differ by more than 7% in absolute magnitude. By contrast, the 6-31g** basis set, an excellent flexible basis set for most purposes, fails in this respect for VCD as expected from the discussion of Table III. Comparing columns four and five of Table VII, one sees that two bands differ in sign of Cotton effect and that the intensities vary considerably in absolute magnitude.

Even more serious is the comparison between columns 4 and 10. The 6-31g** basis set yields the opposite sign of Cotton effect for three transitions and the majority of the Cotton effects where the sign is correctly predicted are in error by 50% or more in absolute magnitude. It should be borne in mind that "correctness" is judged against the 6-31g̃(-2s̃,2p̃,2p̃$_H$) results in the absence of experimental data.

Table IV. Effect of Scaling on 6-31g̃(−2s̃,2p̃,2p̃$_H$) APT Infrared Absorption Intensities (in km/mol)

		geom						
		exptl[b]		6-31g̃(−2s̃,2p̃,2p̃$_H$)			LAKS[c]	
	exptl[a]	1sf	7sf	1sf	3sf	7sf	unscld	scld
				Oxirane				
ν_1 (A_1)	0.21	0.3	1.0	0.5	0.5	0.7	0.05	0.04
ν_2 (B_2)	8.56	9.3	9.3	9.6	9.6	9.6	4.25	4.26
ν_3 (A_1)	63.94	80.5	84.0	81.7	83.8	85.8	72.73	77.89
ν_4 (A_2)		0.0	0.0	0.0	0.0	0.0		
ν_5 (A_1)		2.7	0.4	1.3	1.0	0.6	0.25	1.75
ν_6 (B_1)		7.5	6.9	7.6	7.6	7.4	3.04	3.03
ν_7 (B_2)		0.1	0.0	0.0	0.0	0.0	7.52	7.54
ν_8 (A_2)		0.0	0.0	0.0	0.0	0.0		
ν_9 (A_1)	13.16	12.3	10.6	13.4	11.7	10.0	17.10	10.51
ν_{10} (B_2)	0.34	0.0	0.0	0.0	0.0	0.0	0.00	0.00
ν_{11} (A_1)	1.04	1.4	1.9	1.8	1.8	1.9	0.42	0.38
ν_{12} (B_2)	44.3	35.7	35.7	36.3	36.3	36.3	24.30	24.30
ν_{13} (A_1)	6.04	9.5	9.5	10.0	10.0	10.0	3.11	3.07
ν_{14} (A_2)		0.0	0.0	0.0	0.0	0.0		
ν_{15} (B_1)	36.24	38.1	38.0	39.8	39.8	39.8	42.63	42.61
				2,2,3,3-Tetradeuteriooxirane				
ν_1 (B_1)	0.45	0.3	0.7	0.3	0.3	0.5	0.07	0.07
ν_2 (A_2)		0.0	0.0	0.0	0.0	0.0		
ν_3 (A_1)	34.23	48.5	42.1	42.8	43.8	42.8	50.33	49.28
ν_4 (B_2)	6.76	8.7	8.6	8.9	8.9	8.9	3.64	3.69
ν_5 (B_1)	3.80	7.8	7.5	7.9	7.9	7.8	9.32	9.31
ν_6 (B_2)	0.10	0.0	0.0	0.1	0.1	0.1	0.65	0.58
ν_7 (A_2)		0.0	0.0	0.0	0.0	0.0		
ν_8 (A_1)	23.14	29.1	36.6	34.2	35.6	37.5	13.32	21.27
ν_9 (A_1)	1.69	0.4	0.1	1.3	0.1	0.1	5.37	0.26
ν_{10} (B_2)	0.05	0.2	0.2	0.2	0.2	0.2	0.05	0.07
ν_{11} (A_1)	6.43	7.6	6.9	8.6	7.5	6.6	6.01	3.98
ν_{12} (B_2)	19.89	21.5	21.5	21.9	21.9	21.9	14.19	14.18
ν_{13} (A_1)	7.17	6.8	6.7	7.0	6.9	6.9	2.36	2.16
ν_{14} (A_2)		0.0	0.0	0.0	0.0	0.0		
ν_{15} (B_1)	23.77	27.0	26.9	28.0	27.9	27.9	31.10	30.66

[a] Experimental infrared absorption intensities of oxirane and oxirane-d_4, Nakanaga et al.[14] [b] Experimental geometry, Hirose.[61] [c] Reference 17.

Table V. 6-31g̃(−2s̃,2p̃,2p̃$_H$) Frequencies (in cm^{-1}) of the Deuterio Isotopomers of Oxirane at the Optimized Geometry and Uniform Scaling[a]

band[b]	(*S*)-2-deuterio-oxirane (C_1)	(*S*,*S*)-2,3-dideuterio-oxirane (C_2)	(*S*,*R*)-2,3-dideuterio-oxirane (C_s)	2,2-dideuterio-oxirane (C_s)	(*S*)-2,2,3-trideuterio-oxirane (C_1)
ν_1	699 (A)	653 (B)	632 (A′)	653 (A″)	605 (A)
ν_2	820 (A)	750 (A)	798 (A″)	794 (A′)	744 (A)
ν_3	838 (A)	828 (B)	832 (A″)	806 (A″)	796 (A)
ν_4	890 (A)	872 (A)	832 (A′)	828 (A′)	823 (A)
ν_5	1050 (A)	917 (B)	941 (A′)	964 (A′)	902 (A)
ν_6	1086 (A)	966 (A)	975 (a″)	1037 (A′)	949 (A)
ν_7	1154 (A)	1120 (B)	1093 (A′)	1064 (A″)	971 (A)
ν_8	1156 (A)	1137 (A)	1127 (A″)	1107 (A″)	1039 (A)
ν_9	1243 (A)	1221 (A)	1229 (A′)	1166 (A′)	1128 (A)
ν_{10}	1374 (A)	1339 (B)	1346 (A″)	1284 (A′)	1258 (A)
ν_{11}	1503 (A)	1407 (A)	1405 (A′)	1501 (A′)	1384 (A)
ν_{12}	2214 (A)	2206 (B)	2204 (A″)	2157 (A′)	2154 (A)
ν_{13}	2968 (A)	2221 (A)	2224 (A′)	2277 (A″)	2216 (A)
ν_{14}	3011 (A)	3010 (A)	3006 (A″)	2969 (A′)	2277 (A)
ν_{15}	3050 (A)	3013 (B)	3018 (A′)	3050 (A″)	3012 (A)

[a] Scale factor: 0.814. [b] All frequencies listed in ascending order.

VCD. Effect of Nonuniform Scaling. Columns 7 and 10 compare the effects of nonuniform (7sf) vs uniform (1sf) scaling of the ab initio force constant matrix. While all of the signs are the same and many of the magnitudes are within a few percent, it is clear that scaling the force field has a larger effect on calculated VCD intensities than on IR intensities (Table IV). For reasons discussed above, we lean toward favoring the uniformly scaled results, column 10, but the question of the effect of scaling cannot be definitively answered until more experimental data become available.

VCD. Effect of Model. The APT model of VCD intensities (i.e., magnetic moment by eq 6) was developed by Nafie and co-workers in an effort to provide a model with the same conceptual simplicity as the APT model for IR intensities, using readily available ab initio atomic polar tensors. In the absence of an implementation of the ab initio vibronic coupling theory (VC), it was not clear whether the approximations to VC (eq 9) that enable the derivation of the APT equivalent (eq 6) were justified. Comparison of columns 9 and 10 of Table VII suggests that APT for VCD has little predictive capability, even for sign of Cotton effect. While the signs and relative magnitudes are correctly predicted for the C–H and C–D stretching vibrations (ν_{12}–ν_{15}), 5 of the remaining 11 bands in the mid-IR region are calculated to have opposite signs. We do not recommend use of the APT model for VCD except possibly in the C–H and C–D stretching regions.

VCD. Origin Dependence. Throughout this work, all moments are evaluated at a common origin, namely, the molecular center of mass. The origin dependence of the calculated rotational strengths was examined by explicit recalculation of the results of the last two columns in Table VII at an origin displaced by 0.5 Å in the (1,1,1) direction relative to the center of mass. The

Table VI. APT 6-31g̃(−2s̃,2p̃,2p̃$_H$) Infrared Intensities (in km/mol) of the Deuterated Oxiranes at the Optimized Geometry and Uniform Scaling[a]

band[b]	(*S*)-2-deuterio-oxirane	(*S*,*S*)-2,3-dideuterio-oxirane	(*S*,*R*)-2,3-dideuterio-oxirane	2,2-dideuterio-oxirane	(*S*)-2,2,3-trideuterio-oxirane
ν_1	3.4	0.3	3.2	0.6	0.9
ν_2	23.4	26.4	2.0	49.8	19.1
ν_3	23.0	9.4	6.9	2.1	27.8
ν_4	38.0	28.4	59.5	9.8	8.9
ν_5	4.9	4.8	17.6	24.7	4.6
ν_6	3.2	24.9	0.6	6.4	1.4
ν_7	1.2	2.6	6.4	1.4	27.7
ν_8	1.7	0.2	0.0	4.0	5.2
ν_9	10.8	8.8	10.4	0.0	1.0
ν_{10}	2.2	0.4	0.0	10.3	7.3
ν_{11}	1.3	3.8	3.7	1.0	3.3
ν_{12}	14.4	24.8	12.8	14.6	16.8
ν_{13}	24.4	4.0	15.9	13.8	11.6
ν_{14}	16.0	4.6	16.2	22.9	14.4
ν_{15}	24.0	38.2	26.5	20.1	21.4

[a] Scale factor: 0.814. [b] Values listed in ascending order of corresponding frequencies.

Table VII. 6-31g̃(−2s̃,2p̃,2p̃$_H$) VCD Intensities (in cm/mol) of (*S*,*S*)-2,3-Dideuteriooxirane: Effect of Basis Set, VCD Model, and Choice of Origin[a]

		6-31g**//7sf			6-31g̃(−2s̃,2p̃,2p̃$_H$)//7sf			6-31g̃(−2s̃,2p̃,2p̃$_H$)//1sf		
			VC			VC			VC[c]	
	obsd[b]	APT	eq 8/9	eq 7/9	APT	eq 8/9	eq 7/9	APT	eq 8/9	eq 7/9
ν_1 (B)		−0.2	−19.7	−113.0	5.2	27.9	27.9	4.5	22.2 (14.5)	22.5 (15.3)
ν_2 (A)		54.9	−27.9	−11.1	45.5	24.4	24.2	46.8	15.7 (15.7)	15.6 (15.6)
ν_3 (B)		7.5	−18.8	27.0	0.4	−16.7	−15.6	0.2	−17.5 (−17.5)	−16.5 (−16.5)
ν_4 (A)		−103.6	−44.3	−73.2	−107.2	−87.9	−88.7	−96.9	−48.1 (−48.1)	−48.6 (−48.6)
ν_5 (B)		−37.0	53.2	49.4	−30.4	39.8	37.2	−28.0	52.3 (67.4)	49.1 (63.3)
ν_6 (A)	(−s)	33.5	−93.7	−120.2	37.9	−137.0	−135.2	29.4	−181.8 (−181.8)	−180.2 (180.2)
ν_7 (B)	(+m)	70.3	220.4	13.9	75.3	161.8	163.3	74.8	157.9 (143.6)	159.8 (146.7)
ν_8 (A)		4.4	77.7	158.0	3.4	25.6	17.6	5.0	37.2 (37.2)	28.5 (28.5)
ν_9 (A)	(+s)	−41.6	155.8	−96.0	−24.8	216.6	207.4	−30.3	234.9 (234.9)	226.2 (226.2)
ν_{10} (B)	(−w)	7.0	50.4	254.8	1.7	−12.0	−16.2	1.3	−11.8 (−1.1)	−15.8 (−4.3)
ν_{11} (A)	(−s)	13.5	−316.3	−283.3	−1.4	−241.9	−223.9	−1.4	−261.7 (−261.7)	−243.8 (−243.8)
ν_{12} (B)	(−s)	−108.0	−421.6	−841.9	−73.0	−268.2	−276.6	−72.3	−265.7[d] (−166.8)	−274.0 (−179.2)
ν_{13} (A)	(+s)	137.1	442.0	754.8	88.7	295.0	297.0	88.6	295.4[e] (295.4)	297.5 (297.5)
ν_{14} (A)	(−m)	−235.6	−548.3	−854.4	−146.4	−357.6	−362.2	−145.3	−355.2[f] (−355.3)	−359.8 (−359.8)
ν_{15} (B)	(+s)	229.2	751.5	1222.7	143.8	437.7	450.1	142.5	434.1[g] (432.7)	446.4 (447.8)

[a] Uniform scale factor for all calculations: 0.814. [b] Reference 9; s = strong, m = medium, w = weak. [c] Values in parentheses are recalculated VCD intensities at an origin (0.5 Å, 0.5 Å, 0.5 Å) relative to the center of mass. [d] −330.[10] [e] 323.[10] [f] −813.[10] [g] 937.[10]

results obtained are given in parentheses in Table VII. By symmetry rules, only the VCD intensities corresponding to normal modes of B symmetry are origin dependent. The largest discrepancies arising from the shift of origin occur for modes ν_1, ν_5, ν_{10}, and ν_{12}. Nonetheless, the qualitative features of the predicted VCD spectrum remain unchanged, confirming the relative insensitivity to choice of origin provided factors discussed above are optimal. We expect errors originating from gauge dependence to be minimized if the center of mass of the molecule is chosen as common origin for such VCD calculations.

VCD Intensities for the Chiral Deuteriooxiranes

VCD intensities computed as in column 10 of Table VII are listed in Table VIII for (*S*)-2-deuteriooxirane, (*S*,*S*)-2,3-dideuteriooxirane, and (*S*)-2,2,3-trideuteriooxirane, in the same order as the frequencies and IR intensities in Tables V and VII, respectively. The predicted VCD spectra are simulated in Figures 4, 5, and 8, respectively. The 2,3-dideuterio isotopomer is the most intensely optically active, especially in the C–H and C–D stretching region of the spectrum. The relative intensities and sign ordering observed in the experimental spectrum[8,9] is reproduced very well. Comparison with experiment[8,9] and with the ab initio calculation of Stephens and co-workers[10] is possible in the C–H and C–D stretching regions. Absolute magnitudes of the C–D stretching modes agree well with those of Stephens.[10] However, we predict that the rotary strengths of the two C–H stretches should not be as intense as calculated by Stephens.[10] Band ν_{11} near 1407 cm^{-1} involves scissoring of the CHD groups and stretching of the C–C bond. Band ν_9 near 1221 cm^{-1} involves rocking of the C–H bonds in the CHD plane coupled with ring breathing.

Table VIII. 6-31g̃(−2s̃,2p̃,2p̃$_H$) Vibrational Circular Dichroism Intensities (in cm/mol) of Oxirane and Its Deuterated Analogues at the Optimized Geometry and Uniform Scaling[a]

band	(*S*)-2-deuterio-oxirane	(*S*,*S*)-2,3-di-deuteriooxirane[b]	(*S*)-2,2,3-tri-deuteriooxirane
ν_1	−13.4	22.2	16.8
ν_2	9.7	15.7	36.4
ν_3	70.3	−17.5	−93.1
ν_4	−17.5	−48.1	−17.3
ν_5	−145.5	52.3	54.5
ν_6	−55.0	−181.8 (−s)	−19.4
ν_7	67.5	157.9 (+m)	−103.8
ν_8	127.0	37.2	71.9
ν_9	135.2	234.9 (+s)	82.1
ν_{10}	−162.0	−11.8 (−w)	141.8
ν_{11}	−17.2	−261.7 (−s)	−168.9
ν_{12}	1.7	−265.7 (−s)	−74.5
ν_{13}	51.0	295.4 (+s)	100.0
ν_{14}	−84.5	−355.2 (−m)	1.9
ν_{15}	78.6	434.1 (+s)	34.0

[a] Scale factor: 0.814. [b] Symbols in parentheses refer to experimental spectral features (ref 9); s = strong, m = medium, w = weak.

Compared to the 2,3-dideuterio species, the mono- and trideuterio species have relatively weak VCD in the C–H and C–D stretching region. Indeed two bands have almost no VCD intensity although both are moderately strong in the IR. In the case of the d_3 species, the weak VCD band, ν_{14}, at 2277 cm^{-1} is a strongly

localized antisymmetric stretching motion of the CD_2 group. Such a motion must be associated with a nonzero magnetic dipole transition moment. The weakness of the rotatory strength is probably a consequence of the near orthogonality of the electric and magnetic dipole transition moments.

Further discussion of the origin of the VCD intensities in the three chiral species is deferred until additional data become available. We note in passing that all of the stronger VCD bands in the mid-IR region of all species involve coupling to deformations of the three-membered ring. This may be taken to be substantiating evidence for the ring-current mechanism advocated by Nafie and co-workers.[8]

Conclusions

An ab initio implementation of the vibronic coupling theory of Nafie and Freedman[29] is described and applied to the computation of VCD intensities of (*S*)-2-deuteriooxirane, (*S*,*S*)-2,3-dideuteriooxirane, and (*S*)-2,2,3-trideuteriooxirane. The theory is found to reproduce the spectral features of the (*S*,*S*)-2,3-dideuteriooxirane molecule very well if due consideration is given to the choice of the basis set. The basis set must incorporate derivatives of the normal set of basis functions, a conclusion also reached by others.[44-48] Such a basis set, based on the standard 6-31g set and designated 6-31$\tilde{g}$(-2$\tilde{s}$,2$\tilde{p}$,2$\tilde{p}_H$), is found to yield a geometry for oxirane that is closer to the microwave structure than obtained by optimization with the comparably sized 6-31g** set. Uniform scaling or temperature nonuniform scaling of the 6-31$\tilde{g}$(-2$\tilde{s}$,2$\tilde{p}$,2$\tilde{p}_H$) force constants permits excellent agreement (<1% error) with observed vibrational frequencies of oxirane and tetradeuteriooxirane. Quite satisfactory agreement with the measured IR intensities for these two compounds is also obtained. The effect of nonuniform scaling of the force constants is slightly adverse, suggesting that the ab initio normal modes are somewhat superior to those obtained as a result of adjustments to the force field by the normal procedure.[5,50,53,54] It is not known whether this observation can be generalized to other molecules or to VCD intensities even of chiral oxiranes.

The APT theory of VCD intensities introduced by Nafie and Freedman[28] has been tested against the vibronic coupling theory. Ab initio atomic polar tensors that accurately reproduce the IR spectrum of oxirane and the d_4 species were employed. The APT theory was found to have no predictive capability except possibly in the C-D and C-H stretching region of the spectrum. We recommend against its use.

The full IR spectra of all of the deuterated isotopomers of oxirane and the VCD spectra of all of the chiral species are predicted.

Acknowledgment. We express our gratitude to R. A. Shaw for making his "scaling program" available to us. We thank L. A. Nafie and T. B. Freedman for communicating the VCD data of (*S*,*S*)-2,3-dideuteriooxirane prior to publication and P. J. Stephens for helpful comments on the manuscript. This work was supported by the Natural Sciences and Engineering Research Council of Canada (NSERCC) and in the early stages by a Graduate Scholarship to R.D. from the Killam Foundation. We also thank Supercomputer Services of the University of Calgary for a generous amount of time on the CDC Cyber205 supercomputer.

Synthesis and Characterization of DNA Oligomers and Duplexes Containing Covalently Attached Molecular Labels: Comparison of Biotin, Fluorescein, and Pyrene Labels by Thermodynamic and Optical Spectroscopic Measurements

Joshua Telser,[†] Kenneth A. Cruickshank, Larry E. Morrison, and Thomas L. Netzel*

Contribution from the Amoco Technology Company, Amoco Research Center, P.O. Box 400, Naperville, Illinois 60566. *Received June 24, 1988*

Abstract: A series of oligonucleotides having the base sequence 5'-GCA(C*-L)(T*-L)CAG-3' have been synthesized where C* and T* are respectively a chemically modified cytidine or thymidine base containing a linker arm terminating in either a primary amine or a molecular label (L) such as biotin, fluorescein, or pyrene. Each oligomer contained a maximum of one chemically modified base. Additionally, the corresponding unmodified oligomers and their complementary unmodified strands were also synthesized. The results of absorption and fluorescence measurements as well as melting temperature studies on these oligomers and their corresponding duplexes are described. Duplexes formed from oligomers containing a T* base exhibited normal melting curve behavior, while those containing a C* base in some cases did not. As a result, thermodynamic parameters for duplex formation were determined only for the former cases. Fluorescence quantum yields were also measured for the T* fluorophore-labeled oligomers both as single strands and as duplexes. Both emission quenching and duplex stabilization indicated strong duplex association (perhaps intercalation) by the covalently attached pyrene labels. No such effects were seen in the duplex formed with the fluorescein-labeled oligomer. The results are discussed in terms of the requirements for achieving good hybridization with labeled oligomers, and in the case of the fluorophore-labeled oligomers, high emission quantum yields from their duplexes.

The base-pairing property of oligomeric strands of DNA allows specific recognition of a particular base sequence in a target strand by a complementary base sequence in a probe strand. However, since DNA probe strands do not naturally contain any convenient reporter groups, spectroscopic monitoring of hybridization is difficult except in ideally controlled settings. A method to overcome this problem is to prepare a synthetic oligonucleotide with the desired base sequence that also contains a covalently attached molecule label (or reporter group). This label is selected to be easily detectable. For example, direct spectroscopic observation by optical absorption or emission is possible, or as in the case of biotin as a reporter group, enzymatic methods and colorimetric

* To whom correspondence should be addressed.
[†] Present address: Squibb Institute for Medical Research PO Box 191, New Brunswick, NJ 08903.

0002-7863/89/1511-6966$01.50/0 © 1989 American Chemical Society